ELSEVIER

Surface Science 449 (2000) 191–206

surface science

www.elsevier.nl/locate/susc

# Analysis of terrace width distributions on vicinal copper surfaces using the 'Wigner surmise': comparison with Gaussian approach

M. Giesen [a], T.L. Einstein [b,*]

[a] *Institut für Grenzflächenforschung und Vakuumphysik, Forschungszentrum Jülich, 52425 Jülich, Germany*
[b] *Department of Physics, University of Maryland, College Park, MD 20742-4111, USA*

Received 22 July 1999; accepted for publication 17 December 1999

**Abstract**

We have analyzed the terrace width distribution on a large number of Cu (100) and (111) vicinal surfaces using the standard Gaussian fit as well as by using an alternative analytical distribution, which comes from the perspective of fluctuation phenomena and is referred to as the generalized Wigner surmise. The chief motivation is to extract optimally the strength $A$ of the elastic repulsion between steps. Both methods provide generally consistent estimates of the variance. We find the Wigner approach provides a viable alternative to the standard Gaussian approach. We review competing views on the proportionality constant relating $A$ to the inverse square of the variance of a Gaussian fit; the experimental range of data seems to straddle the range over which various values are optimal. The previously suggested method for analyzing skewness proves unsatisfactory with actual data. By comparing data for different temperatures and misorientations with predictions based on scaling, we illustrate the difficulties of obtaining quantitative information about $A$. © 2000 Elsevier Science B.V. All rights reserved.

*Keywords:* Copper; Equilibrium thermodynamics and statistical mechanics; Stepped single crystal surfaces; Surface structure, morphology, roughness, and topography; Vicinal single crystal surfaces

## 1. Introduction

By examination of the *quantitatively measurable* terrace width distributions (TWDs) on vicinal surfaces one can extract information about the interaction between the steps. The typical analysis procedure makes use of the mean-field-like Gruber–Mullins expression when there are no energetic interactions between the steps [1] and a similarly derived Gaussian approximation when these interactions are strong [2]. There are problems with this standard method for both small and large interactions. For small interactions, the fundamental assumption that the potential can be quadratically expanded — ultimately that the fluctuations of a step are small compared with the mean spacing — breaks down. Then the TWD can no longer be determined reliably in this framework. In the other extreme, there are more subtle issues (to be discussed shortly) on how to gauge the repulsion strength from the width of the Gaussian.

In a recent paper, Einstein and Pierre-Louis (EP) observed that the distribution associated with the so-called generalized Wigner surmise (hereafter

* Corresponding author. Fax: +1-301-314-9465.
*E-mail addresses:* m.giesen@fz-juelich.de (M. Giesen), einstein@physics.umd.edu (T.L. Einstein)

0039-6028/00/$ - see front matter © 2000 Elsevier Science B.V. All rights reserved.
PII: S0039-6028(99)01254-6

GWD, for 'generalized Wigner distribution'), arising from random-matrix theory, could describe these equilibrium fluctuations, as it does many other fluctuation phenomena in physics [3]. This recognition relies on the intimate relation of the problem of interacting steps to that of fermions in one spatial dimension. The simple analytic expression provides an excellent approximation of the exact distribution for the three particular interactions for which the problem can actually be solved, as well as for other values in that range of interactions.

This finding proves particularly timely, since in recent years two groups have taken issue with how the Gruber–Mullins approach estimates the strength of the interstep interactions — particularly for large repulsions — from the variance of a Gaussian fit to the TWD [4–8]. While still affirming that the variance of the Gaussian is proportional to the inverse square root of this strength, these papers argue that the prefactor should be considerably larger, by a factor somewhat below two (but by a different factor for the two groups); thus, the interaction strength obtained from the Gruber–Mullins Gaussian expression underestimates the actual interaction strength considerably, at least for large strengths.

All these Gaussian methods neglect the TWD's skewness, which is considerable for weak interactions — at which none of these Gaussian approximations are suitable. In contrast, the GWD does allow for skewness within an expression almost as simple as a Gaussian and has been applied successfully to study the fluctuations of a broad range of problems in many fields.

EP [3] offered a number of ideas on how to approach experimental data via the Wigner surmise, but did not actually test them. In this paper we describe the first attempt to apply straightforwardly and systematically this formula and viewpoint to a large number of vicinal surfaces of copper at various temperatures. The data sets include both good experimental data and poorer results; they span the range from the upper end of weak step repulsions to moderately strong interactions. We can thus assess under a wide range of conditions which analysis procedures are viable and offer suggestions on how best to extract information from experimental data.

We wish to address the following set of questions. Under which conditions does the Gaussian or the Wigner expression provide the better fit of experimental TWDs? For a particular data set, how well does the variance associated with the GWD fit compare with that immediately emerging from the Gaussian fit? How much difference is there among the various estimates of the interaction strength for any particular actual data set? Can consistent information about interactions also be extracted from the skewness of the TWDs? How do the various errors innate in experimental data confound the extraction of accurate information from each type of fit?

The paper is organized as follows. In Section 2 we describe the experimental set-up. We provide the reader with the essential theoretical ideas in Section 3. Then Section 4 follows with a presentation and discussion of the analysis of experimental results for various copper vicinal surfaces using both the standard Gaussian approximation and the GWD. Section 5 summarizes our findings and gives conclusions.

## 2. Experimental

The experiments were performed in a standard ultrahigh vacuum chamber with a base pressure of $5 \times 10^{-11}$ mbar. Our variable-temperature scanning tunneling microscope (STM) is of the Besocke type. The experimental set-up and the sample cleaning are described in detail in previous publications [9,10].

We used six different samples. Three of them were vicinal to the Cu (001) plane: Cu (117), (1 1 13) and (1 1 19).[1] These crystal planes have miscut angles of 11.4°, 6.2° and 4.3° respectively

[1] It should be noted that these vicinal orientations are not facets but correspond to rough parts of the equilibrium crystal shape. As such, there is no physical importance associated with the actual orientation having $\langle \ell \rangle$ simply related to $a_\perp$, as it would be on a facet plane. (E.g. for close-packed steps on a {100} surface, this simple relation is that $\langle \ell \rangle / a_\perp$ be a positive integer plus $\frac{1}{2}$.) In other words, the Miller indices can be viewed as approximate.

about the dense [$\bar{1}10$]-direction. The mean step separation $\langle\ell\rangle$ is 8.9 Å [corresponding to $3.5a_{\perp}^{(001)}$, where $a_{\perp}^{(001)}=2.55$ Å is the spacing between $\langle 110\rangle$ (close-packed) atomic rows on the (001)-oriented copper terrace], 16.6 Å [$6.5a_{\perp}^{(001)}$] and 24.2 Å [$9.5a_{\perp}^{(001)}$] respectively. The terraces are separated by parallel single-layer {111}-microfacet steps along [110]. The other three surfaces are vicinals to the Cu (111) plane. Their miscut angles are 12.75°, 3.05° and 2.49° about the [$\bar{1}\bar{1}2$] direction. These surfaces have orientations (11 7 7), (19 17 17) and (23 21 21) respectively.[1] The samples consist of parallel single-layer A-type [{100}-microfacet] steps along $\langle 110\rangle$.[2] The mean terrace widths between adjacent steps are 9.2 Å [corresponding to $4.17a_{\perp}^{(111)}$, where $a_{\perp}^{(111)}=2.21$ Å is the spacing between close-packed rows, so appropriate for a (100)-step on a (111)-surface], 39.1 Å [$17.67a_{\perp}^{(111)}$] and 47.9 Å [$21.67a_{\perp}^{(111)}$] respectively.[3] The accuracy of the quoted miscut angles for all surfaces is within 0.1°.

In our experiments, the concentration of pinning sites on the surface was lower than $10^{-7}$ per atom. For the analysis, we have chosen STM images obtained from areas free of visible residual contamination. A measured TWD was accepted for further analysis only when the average step density found from the distribution was consistent with the nominal step density given by the miscut angle of the surface. Fig. 1 shows STM images of (a) Cu (11 7 7) at 296 K and (b) Cu (23 21 21) at 303 K. The scan widths are 240 Å and 760 Å respectively. STM images of the stepped Cu (001) surfaces were published previously [12].

We used a computer code in order to determine the step–step distance distributions. This code searches for the maximum slope in a spline fitted to the gray-scale values of each scan line perpendicular to the step edges. For each distribution we analyzed a total step length of 5–17 μm taken from 10–40 STM images from different areas of the sample.

## 3. Theory

### 3.1. Review of fermion mapping and 'mean field'

In the downstairs direction on a vicinal surface there is just one characteristic length, the average $\langle\ell\rangle$ of the step spacings $\ell$. Hence, it is natural to use as the independent variable $s\equiv\ell/\langle\ell\rangle$ to plot the TWD $P(s)$. This distribution must be normalized, and by construction it has unit mean. In general there is a repulsion between the steps of the form $A/\ell^2$, due to elastic or dipolar forces, and there is always an entropic repulsion — because steps cannot cross — that obeys the same power-law decay. Then there are three energy-related quantities that determine the TWD (below the roughening temperature of the terraces): (1) the thermal energy, $k_BT$, which produces the fluctuations of the steps; (2) the stiffness of each step $\tilde{\beta}$ [2], which opposes bending of the step and has units of energy per length;[4] (3) the strength $A$ of the repulsion, which has units energy × length. There is only one dimensionless combination that can be formed: we define

$$\tilde{A}\cong\frac{A\tilde{\beta}}{(k_BT)^2}. \tag{1}$$

Since steps do not start, end, or cross, the set of their configurations is equivalent to world lines ('time-lapse photos') of fermions evolving in one spatial dimension [i.e. $(x, y)$ plots can be viewed as $(x, t)$ plots]. When $A=0$, the world lines are those of free fermions. The venerable Gruber–Mullins approximation fixes the two neighboring steps of a fluctuating ('active') step to be straight and separated by twice the average spacing [1].

[2] For the analysis, we choose exclusively vicinals with A-steps because a previous study of Cu (997) (which consists of parallel B-type steps) showed that these surfaces are unstable and restructure into other facet orientations [11].

[3] In Ref. [10], erroneously different values for the nominal $\langle\ell\rangle$ were given. The analysis of the TWDs presented there, however, is not altered.

[4] Equivalently, $\tilde{\beta}$ can be written as $k_BTa_{\parallel}b^{-2}$, where $b^2$ is the diffusivity [2] and $a_{\parallel}$ the lattice spacing along the step. Assuming that the energy of kinks is proportional to the kink length, the diffusivity can be expressed in terms of the kink formation energy $\epsilon$ [13,14]: $b^{-2}=2a_{\perp}^{-2}\sinh^2(\epsilon/2k_BT)$, where $\epsilon=128\pm3$ meV for Cu (100) vicinals [15] and $\epsilon=113\pm12$ meV for (111) vicinals [16].

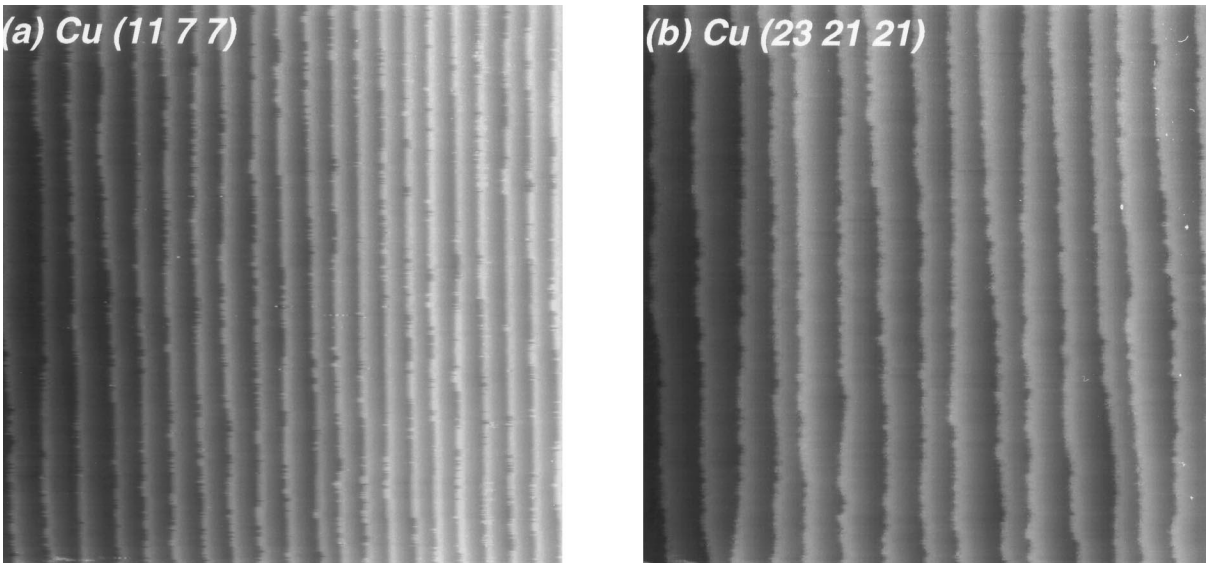


Fig. 1. STM images of (a) Cu (11 7 7) at $T=296$ K and (b) Cu (23 21 21) at $T=303$ K. The scan widths are 240 Å and 760 Å respectively. The monatomic steps run from top to bottom, and the surface height increases from left to right.

Since the TWD corresponds to the ground-state density in the corresponding quantum problem, we find from recollection of the standard problem of a particle in a 1-D box that

$$P(s)=\sin^2\left(\frac{\pi s}{2}\right). \tag{2}$$

Analytic approximants containing large numbers of elementary functions offer an arbitrarily accurate representation of the exact result [17], but can be inconvenient to use.

When there are strong repulsions between the steps, so that the motion of each step tends to be confined near its mean position, a Gruber–Mullins argument shows that $P(s)$ can be approximated by a Gaussian [1,2]

$$P(s)=\frac{1}{\sigma\sqrt{2\pi}}\,\mathrm{e}^{-[(s-1)^2/2\sigma^2]}, \tag{3}$$

where the variance $\sigma^2$ is given by

$$\sigma^2=(48\tilde{A}_{\mathrm{G}})^{-1/2}, \tag{4}$$

if only nearest neighbors are considered and by

$$\sigma^2=\left(\frac{15}{8\pi^4\tilde{A}_{\mathrm{G}}}\right)^{1/2}\cong(51.95\tilde{A}_{\mathrm{G}})^{-1/2} \tag{5}$$

if all steps are included. [Since the coefficient of $\tilde{A}_{\mathrm{G}}$ in Eq. (5) is about 8% larger than that in Eq. (4), the estimate of $\tilde{A}_{\mathrm{G}}$ from Eq. (5) is about that much smaller than that from Eq. (4), i.e. assuming just nearest-neighbor interactions. The subscript G serves as a reminder that $\tilde{A}_{\mathrm{G}}$ is determined from the Gaussian expression, Eq. (3).]

### 3.2. The GWD

Most of the above is well known, as is the existence of exact solutions for $\tilde{A}=2$, 0, and $-\frac{1}{4}$ [18]. (These three exceptional cases correspond to special cases of repulsive, vanishing, and attractive energetic interactions between steps, as depicted in Ref. [17]. E.g. for steps on a Cu(001) vicinal surface at room temperature, the case $\tilde{A}=2$ corresponds to a repulsive interaction constant $A=$ 1.8 meV Å.) The new idea from random-matrix theory [19,20] is that fluctuations should exhibit certain universal behavior (ultimately determined by the symmetry of the couplings of the states, in a way that does not have any obvious physical interpretation in the present context). According to the generalized Wigner surmise, the distribution of fluctuations can be approximated by [3] the

GWD form:

$$P_\varrho(s) = a_\varrho s_\varrho \exp(-b_\varrho s^2). \quad (6)$$

The exponent $\varrho$ is related to $\tilde{A}_W$ — the subscript W denoting that $\tilde{A}$ is estimated using the GWD given in Eq. (6) — by[5]

$$\varrho = 1 + \sqrt{1 + 4\tilde{A}_W} \text{ or } \tilde{A}_W = (\varrho - 2)\varrho/4. \quad (7)$$

Thus, $\varrho$ provides an alternate, albeit non-linear, way to describe the strength of the dimensionless interaction.

The constants $a_\varrho$ and $b_\varrho$ are determined by the two conditions of normalization and unit mean respectively. Owing to the simple analytic form of the GWD [Eq. (6)], these two $\varrho$-dependent constants can be expressed explicitly in terms of Gamma functions:

$$b\varrho = \left[\frac{\Gamma\left(\frac{\varrho+2}{2}\right)}{\Gamma\left(\frac{\varrho+1}{2}\right)}\right]^2$$

and

$$a_\varrho = \frac{2b_\varrho^{(\varrho+1)/2}}{\Gamma\left(\frac{\varrho+1}{2}\right)} = \frac{2\left[\Gamma\left(\frac{\varrho+2}{2}\right)\right]^{\varrho+1}}{\left[\Gamma\left(\frac{\varrho+1}{2}\right)\right]^{\varrho+2}}. \quad (8)$$

These two constants turn out to have a rather linear dependence on $\varrho$. For example, the expansions about $\varrho = 4$

$$b_\varrho \cong 2.2635 + 0.4971(\varrho - 4) + 0.0006(\varrho - 4) + O(\varrho - 4)^3, \quad (9)$$

$$\ln a_\varrho \cong 2.4508 + 0.6060(\varrho - 4) - 0.0111(\varrho - 4)^2 + 0.0015(\varrho - 4)^3 - 0.0002(\varrho - 4)^4 + O(\varrho - 4)^5$$

approximate $b_\varrho$ and $\ln(a_\varrho)$ excellently (to within 0.1% and $\sim 0.3\%$ respectively) when $2 \le \varrho \le 8$.

Eq. (6) [supplemented with Eq. (8)] represents an interpolation scheme between the three special cases to which it reduces [the ('ungeneralized') Wigner distributions] at the values 1, 2, and 4 for $\varrho$ (or $-\frac{1}{4}$, 0, and 2 for $\tilde{A}_W$) for which the exact solutions occur. At these three calibration points the Wigner expressions $P_1$, $P_2$ and $P_4$ [Eq. (6)], though quite simple analytically, provide remarkably accurate — at the percent level — approximations of the corresponding exact distributions. The free fermion case ($\tilde{A} = 0$, $\varrho = 2$) was illustrated in Ref. [3]. In Fig. 2 we show the corresponding curves for the case $\varrho = 4$ (or, equivalently, $\tilde{A} = 2$), which is a repulsive moderately strong energetic interaction.

For values well beyond $\varrho = 4$ (i.e. strong step repulsion), the Wigner form can no longer be justified as an interpolation scheme. However, Forrester [21] showed (for even values of $\varrho$, extended to rational values by Haldane [22] and Ha [23]) that the leading (small-$s$) behavior of the exact TWD is proportional to $s^\varrho$ but with a prefactor somewhat different from $a_\varrho$, as given in Eq. (8). For $2 \le \varrho \le 4$, the prefactors agree to within

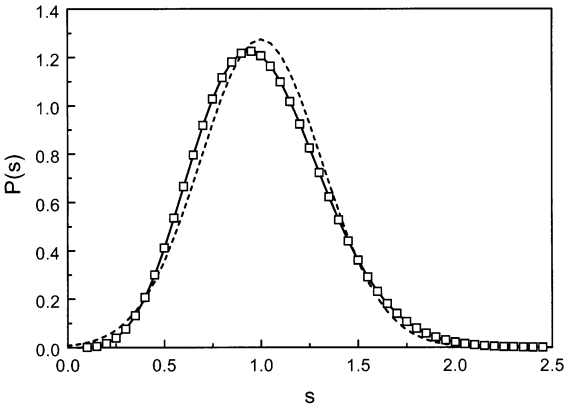


Fig. 2. $P(s)$ versus $s \equiv \ell/\langle\ell\rangle$ for the exactly soluble case $\tilde{A} = 2$. The small squares, representing an accurate numerical implementation of the exact solution, was generated using a code kindly provided by N.C. Bartelt, which he had developed to produce fig. 5 of Ref. [17]. The standard Gruber–Mullins-like Gaussian approximation is given by the dashed curve. The Wigner distribution for this case, $P_4(s)$, is the solid curve; it is visually indistinguishable at this scale from the exact solution.

[5] Eq. (7) follows from inspection of the Sutherland Hamiltonian [18], which describes interacting spinless fermions on a large ring. To our knowledge, there is no intuitive explanation for the profound connection between this Hamiltonian and the random-matrix results underlying Wigner's surmises.

1.5%, whereas $a_\varrho$ is about 10% above the exact value for $\varrho = 30$.

To make connections to Gaussian analyses and to gauge skewness, we study the moments of $P_\varrho(s)$. In this problem it is arguably more convenient [3] to compute $n$th-order moments of the TWD $P_\varrho(s)$ about the origin ($\mu'_n$) than about the mean ($\mu_n$):

$$\mu'_n(\varrho) = \int_0^\infty s^n P_\varrho(s)\, \mathrm{d}s. \tag{10}$$

Specifically, the second moment $\mu'_2$ takes the form

$$\mu'_2(\varrho) = \frac{\varrho + 1}{2b_\varrho}. \tag{11}$$

In dealing with experimental data, one typically seeks the standard deviation $\sigma$ (or the variance $\sigma^2$) of the TWD. For all distributions with unit mean [including $P_\varrho(s)$]

$$\sigma = \sqrt{\mu'_2 - 1}. \tag{12}$$

### 3.3. Recent alternative interpretations of Gaussian width

The Gaussian distribution has been the standard fitting function for analyzing TWDs, not only for its analytic simplicity but also because it can be derived readily from physically plausible assumptions. The traditional Gruber–Mullins approach starts from a mean-field-like viewpoint. Recently, starting from different perspectives, two groups have re-derived Gaussian behavior for the TWDs of vicinal surfaces. Since they make different fundamental approximations, however, the detailed relationship between the width of the Gaussian and $\tilde{A}$ differ notably. In other words, just because one can fit a TWD well with a Gaussian does not mean one has an unambiguous way to estimate $\tilde{A}$. In this section, we provide a quick overview of the various Gaussian approximations and catalog their predictions. The goal is to elucidate the distinction between the schemes. Readers who are new to the subject, or who are disinterested in the controversy about gauging interaction strength from Gaussian width, can skip the remainder of this subsection, Table 1, and the consideration in Section 4 of cols 9, 10, 16, and 17 in Table 2.

As noted in the Section 1, the Grenoble group [4,5] argues that the variances given in Eqs. (4) and (5) are too small in the limit of large step repulsions. At the core of their argument is the observation that the GM approach determines the variance of the TWD from the fluctuations of a *single* 'active' step, the neighboring steps being straight/rigid. If *both* steps bounding a terrace are allowed to fluctuate independently, then the variance of the TWD should be the *sum* of the

Table 1
Coefficients for different approximation methods, to extract interaction strength from the variance of a Gaussian fit. NN denotes that just the steps bounding a terrace ('nearest neighbors') interact [with strength $A$/(terrace width)$^2$], and 'all' indicates that all steps interact in this way. The Saclay and modified Grenoble schemes use $\sigma^2 = \kappa_X \varrho_X^{-1}$ [Eq. (13)] followed by $\tilde{A}_X = \varrho_X(\varrho_X - 2)/4$, whereas the Gruber–Mullins and Grenoble schemes use $\sigma^2 = (k_X \tilde{A}_X)^{-1/2}$ [a generalization of Eqs. (4) and (5)]. As discussed in the text, for asymptotically strong repulsions, either equation can be used; the entries in parentheses are applicable in that limit. Likewise, the limiting values for the GWD are included for comparison

| Model | Approximation | Ref. | Label $X$ | NN/all | $\kappa_X$ | $K_X$ |
|---|---|---|---|---|---|---|
| Gruber–Mullins | Single active step | [1,2] | G | NN | (0.289) | 48 |
| | | | | all | (0.277) | $8\pi^4/15 \cong 51.95$ |
| Grenoble | Entropy of interaction completely neglected | [4,5] | E0 | NN | (0.520) | 14.80 |
| | Independent steps | | | all | (0.475) | 17.75 |
| Grenoble, modified | Entropy of int'n included in average way | [3] | E | NN | 0.520 | (14.8) |
| | | | | all | 0.475 | (17.7) |
| Saclay | Continuum roughening theory | [6–8] | R | all | $4\pi^{-2} \cong 0.405$ | (24.4) |
| Wigner | Wigner surmise | [3,19,20] | W | all | (1/2) | (16) |

variances of the fluctuations of each step, with corrections for correlations of their motion. Thus, if the two steps fluctuate *independently*, the variance of the width of the enclosed terrace should be *twice* that obtained from the GM picture. On closer examination, the motion of neighboring steps is anticorrelated.[6]

It has long been known (but perhaps not widely appreciated) that the contribution of the entropic repulsion *decreases* with increasing energetic repulsion. Physically, the latter repulsion diminishes the chance of neighboring steps approaching each other, where the non-crossing condition underlying the entropic repulsion becomes significant. Thus, in the limit of very strong energetic interstep repulsions, the Grenoble group argues that entropic repulsions between the steps become inconsequential. By neglecting entropic repulsions entirely, the Grenoble group can compute the reduction due to anticorrelations of fluctuations from the enhancement (relative to Gruber–Mullins) factor of two for independently fluctuating steps. The basic form of the variances remains as in Eqs. (4) and (5): $\sigma^2=(k_X\tilde{A}_X)^{-1/2}$, where the subscript $X$ gives a mnemonic for the employed analysis scheme (G for Gruber–Mullins Gaussian; E0, denoting zero entropy, for the Grenoble group's approximation). For nearest-neighbor and all steps interacting, the variance should be increased by factors of 1.801 and 1.711, thereby leading to smaller values of $k_{E0}$ than $k_G$, as indicated in Table 1.

EP [3] showed that estimates of $\sigma^2$ based on this idea could be extended to systems with weaker energetic interactions by including entropic repulsions in an average way (instead of neglecting them completely [4,5]). This improvement is achieved readily via replacing the dimensionless interaction strength $\tilde{A}$ by an effective value $\tilde{A}_{\rm eff}\equiv(\tilde{A}+\frac{1}{4})[1+(4\tilde{A}+1)^{-1/2}]^2$, which is obtained from the cubic term of the expansion of the projected free-energy of a vicinal surface as a function of misorientation slope. (The difference between $\tilde{A}_{\rm eff}$ and $\tilde{A}$ is thus an average contribution of entropic repulsion to the free energy; this contribution decreases monotonically as $\tilde{A}$ increases, consistent with comments in the preceding paragraph.) By comparison with the first of Eq. (7), the effective value is just $\varrho^2/4$. In other words, after substituting the effective for the 'bare' energetic repulsion, one finds $\sigma^2=(k_X\varrho^2/4)^{-1/2}=\kappa_X/\varrho$, where $\kappa_X=2k_X^{-1/2}$. This expression for the variance can be inverted to provide an estimate $\varrho_X$, $X=$E, for the variance and dimensionless interaction based on this modified approximation of the entropic contribution:

$$\varrho_X=\frac{\kappa_X}{\sigma^2};\quad \tilde{A}_X=\frac{\varrho_X(\varrho_X-2)}{4}. \tag{13}$$

Specific values for $\kappa_E$ are given in Table 1. For comparison, for large $\tilde{A}$, the variance of the Wigner distribution becomes asymptotically $(2\varrho)^{-1}$. However, for physical values of $\tilde{A}$, $\kappa_E[1+\sqrt{(1+4\tilde{A})}]^{-1}\equiv\kappa_E/\varrho$ is larger than $\sigma_W^2$ from Eq. (11) [with Eq. (8) and then Eq. (12)] by about 4% at $\varrho=8$, rising to about 10% at $\varrho=5$. (For comparison, at these two values of the dimensionless interaction, $\sigma_G^2$ is less than $\sigma_W^2$ by 30% and 17%, respectively.)

All the approaches discussed so far make a continuum approximation along the 'time-like' $y$ direction but maintain discrete steps. By making a continuum approximation in the $x$ direction as well, and invoking correlation functions from roughening theory, the Saclay group [6–8] argued that the variance is $(4/\pi^2)[1+\sqrt{(1+4\tilde{A})}]^{-1}$, which is also of the form $\kappa_R/\varrho$, with $\kappa_R=4/\pi^2$ somewhat smaller than $\kappa_E$. Using $X=$R in Eq. (13), we find an estimate $\varrho_R$ based on this perspective, with the subscript R as a reminder of the roots of this approach in roughening theory.

In summary, the conclusion that experimental TWD data are well described by a Gaussian does not mean that the dimensionless interaction strength is uniquely determined. There are several competing ways to proceed to extract $\tilde{A}$, and which is best evidently depends on how big $\tilde{A}$ actually is.

### 3.4. Skewness

A distinctive feature of the Gaussian distribution Eq. (3) is that the distribution is symmetric about the mean. Although this description is satis-

[6] In the Gruber–Mullins picture, the anticorrelation is complete since the sum of neighboring terrace widths add to twice the average spacing, $2\langle\ell\rangle$.

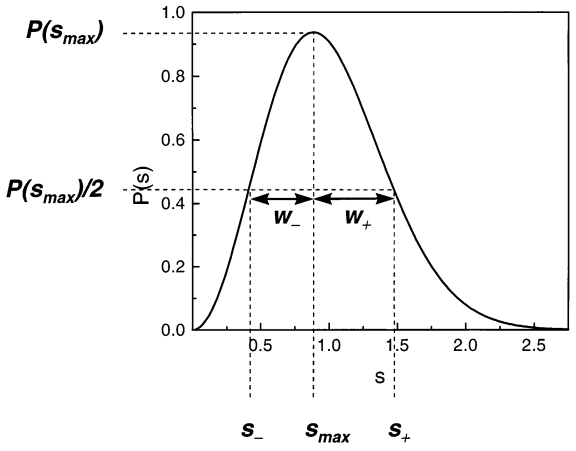


Fig. 3. Schematic to illustrate the parameters to study the asymmetry in the half widths of the TWD. The abscissa of the peak is denoted $s_{\max}$, and the two values of $s$ at which the TWD has half this peak height are denoted $s_+$ and $s_-$. The skewness is a measure of how much the half width $w_+ \equiv s_+ - s_{\max}$ exceeds $w_- \equiv s_{\max} - s_-$.

factory for strong repulsions, it obviously is not good as one approaches the free-fermion limit [a noteworthy shortcoming of Eq. (2)!]. The standard way to quantify the asymmetry is to compute the skewness $\alpha_3$, defined in terms of the third moment about the origin ($\mu_3'$) as [3]

$$\alpha_3 \equiv \frac{\mu_3}{\sigma^3} = \frac{\mu_3' - 1}{\sigma^3} - \frac{3}{\sigma} \text{ where } \mu_3' = \frac{\rho+2}{2b_\rho} = \frac{\rho+2}{\rho+1}\,\mu_2'. \tag{14}$$

Ref. [3] suggested that $\varrho$ and/or $\tilde{A}$ could be determined readily by fitting separately the second and the third moments of the distribution. This proposal turns out not to work well with actual data. The moments are too sensitive to the errors in the measured distribution and the discreteness of the possible terrace widths.

Plummer [24] in turn suggested assessing the skewness more directly by gauging the asymmetry of $w_+$ and $w_-$, the half widths (hw) at half maximum, as depicted in Fig. 3.[7] For moderate values of the dimensionless interaction strength, i.e. $1 \le \tilde{A} \le 6$, the skewness can be well approximated by [3]

$$\alpha_3 \cong 5\,\frac{w_+ - w_-}{w_+ + w_-}. \tag{15}$$

While assessing the asymmetry of the half widths proves more practicable, the experimental TWD data must be suitably smoothed before invoking Eq. (15). In the present analysis we explored two different fits to smooth functions. Initially, we approximated the experimental TWDs by a cubic polynomial in the normalized terrace width $s$ using just the data in the range $s_{\max} - w_- \le s \le s_{\max} + w_+$.[8] This procedure yielded unreasonable results. Instead, to optimize the likelihood of capturing the intrinsic shape of the TWD, we fitted the TWDs to an expression of the form in Eq. (6), but taken as a *three*-parameter expression, i.e. with $a_\varrho$, $b_\varrho$, and $\varrho$ treated as *free* rather than interrelated parameters. Thus, the only savings over a full fit to $P_\varrho(s)$ of Eq. (6) are that one does not need to deal with the analytic expressions for $a_\varrho$ and $b_\varrho$. Viewed conversely, the GWD is arguably the simplest analytic expression that properly captures the innate asymmetry of TWDs.

## 4. Results

Fig. 4 shows TWDs measured on a Cu (1 1 13) surface at three different temperatures. The length scales of the experimental distributions are normalized with respect to the experimentally determined mean terrace widths in each specific measurement. In other words, $\langle \ell \rangle$ is adjusted so that the first moment $\mu_1'$, computed from the discrete version of Eq. (10), is unity. Since our vicinal surfaces are not facets, the nominal value of $\langle \ell \rangle$ given by the misorientation angle may differ from the value of $\langle \ell \rangle$ of the measured region of the sample. (Indeed, such variations are to be expected, and the size of the fluctuations can be quantitatively characterized; see footnote 7 of EP [3].) The value of $\varrho$

[7] In prose, let $s_{\max}$ denote the value at which (a smooth fit to) the experimental TWD takes its maximum, and $w_+$ and $w_-$ are the differences between $s_{\max}$ and the values $s_\pm = s_{\max} \pm w_\pm$ above and below $s_{\max}$ respectively at which the smoothed TWD is half of $P(s_{\max})$; i.e. $P(s_{max} \pm w_\pm) = \frac{1}{2}\,\mathrm{P(s}_{max})$.

[8] The thinking underlying this approach is that the relative errors in the data are smaller in the larger values.

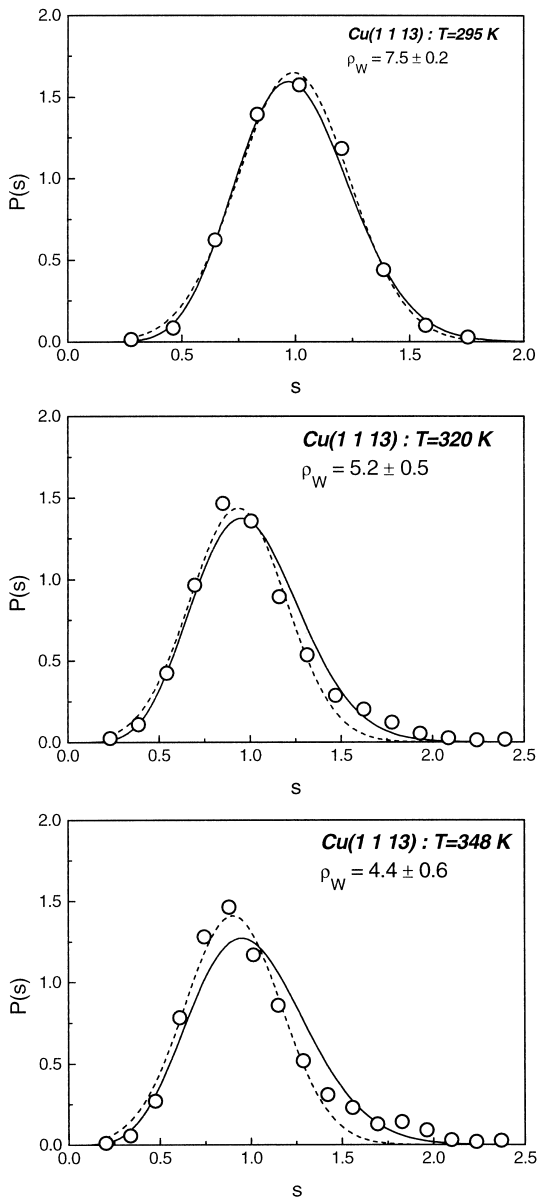


Fig. 4. TWD (indicated by circles) measured for Cu (1 1 13) at different temperatures. The solid curves are fits to the GWD [Eq. (6)] with respect to the single parameter $\varrho$. The dashed curves are fits to a Gaussian.

determined by a fit to the GWD depends sensitively on this scale factor. Differences of less than $a_\perp/2$ between the actual and the assumed mean terrace width introduce errors of 15% into the analysis. For differences of order $a_\perp$, errors in $\varrho$ up to 50% occur (corresponding to 25% errors in $\sigma$).

By treating the Wigner fit as a *two*-parameter fit, in which the length scale $\langle \ell \rangle$ is adjusted along with the exponent $\varrho$, we have been able to deal with these troublesome cases [25]. Since the goal of the present paper is to explore the consequences of conventional, straightforward analysis, we defer presentation of the details of this process [25]. With respect to a simple determination of the variance of the distribution, the Gaussian analysis is less sensitive to deviations of the mean value from the nominal terrace width. (Again, details are deferred to Ref. [25].) Here, deviations of order $a_\perp/2$ still provide results stable to within 5%.

The interaction strength $A$ is relatively independent of $T$, whereas $\tilde{\beta}$ decreases moderately [like $T\exp(\epsilon/k_BT)$, referring to Footnote 4] with increasing $T$ over the relevant thermal range. Hence, $\tilde{A}$ decreases strongly with $T$. Thus, study of the same sample at several different, increasing temperatures provides a scan in $\tilde{A}$ from high to low values, even though $A$ is essentially constant.

For relatively low $T$, the experimental distribution is approximately symmetric. In the top panel of Fig. 4, both the Wigner (solid curve) and the Gaussian (dashed curve) model provide excellent fits to the data. At low temperatures the value of $\varrho$ determined using the GWD is relatively large ($\varrho_W = 7.5$ at 295 K).[9] With increasing temperature, the asymmetry of the step–step distance distribution increases, and the value of $\varrho$ correspondingly

[9] For Cu(1 1 19) around room temperature, broad distributions were observed that could not be described by a repulsive interaction potential [9,26]. Accordingly, it was proposed that attractive step–step interactions may be responsible. In Ref. [9], however, the TWD was found to be well described by (just) a repulsive interaction potential above room temperature. It is still controversial as to whether the strange TWD on Cu(1 1 19) at room temperature arises from attractive interactions between steps. Another intriguing possibility is that one is seeing incipient low-temperature facetting between (100) and (111): Frenken and Stoltze recently proposed [27] that such facetting instabilities might be common at low-enough temperature, but that the vicinal surfaces are stabilized at higher temperatures by the vibrational entropy of step edges. For this scenario to be operative, however, there must be some subtlety, since the facetting instability should occur first (i.e. at highest temperature) for the more misoriented samples, (1 1 7) and then (1 1 13), in the most straightforward view.

decreases ($\varrho_W = 4.4$ at 348 K). Though the Gaussian distribution still describes decently the data in the vicinity of the distribution peak, it fails in the range of large step separations. On the other hand, the Wigner expression gives a slightly less accurate accounting in the range of the peak, though it fits the range of large terrace widths reasonably well. From a formal statistical perspective, the $\chi^2$ for the 35 cases we have studied is higher (i.e. worse) for the Wigner fit than the Gaussian fit in two-thirds of the cases, but rarely by more than a factor of two. (Actually, this comparison is heavily biased against the Wigner expression, since the Gaussian fit used here to obtain $\sigma$ allows three adjustable parameters: the peak center and the prefactor in addition to the width.)

For cataloging behavior, we find it convenient, if perhaps imprecise, to divide the TWDs into three groups based on a visual assessment of their 'quality': 'good' data changes height essentially monotonically below the peak and again above it; there are no dips, humps, or double peaks, and there is minimal scatter in the data points. Thus, the data are well described by the fitting functions. Data that are 'okay' have more scatter, with small dips and peaks introduced by variations (within the limits of the general error margin) of single data points. The remaining TWDs, called 'poor', have double-peaks or humps at large $s$; correspondingly, the position of the (prime) peak occurs noticeably below $s = 1$, even when the peak is fairly narrow and the skewness minimal. As described in more detail in Ref. [25], fits to the Wigner expression can be improved considerably by simultaneously adjusting $\varrho$ and the characteristic length by which $\ell$ is scaled to get $s$. In a Gaussian fit with just the single adjustable parameter $\sigma_G$ (fixing the peak center at $s = 1$), the resulting values for $\sigma_G$ (and so for $\tilde{A}_G$ and $A_G$) are not changed significantly for 'good' data, and the $\chi^2$ roughly doubles. For 'poor' data, the $\chi^2$ rises by nearly an order of magnitude as the standard deviation increases by about 10%, thereby decreasing $\tilde{A}_G$ and $A_G$ by about 40%.) The $\sim 30\%$ of cases in which the single-parameter Wigner fit has lower $\chi^2$ occur often but not always at higher temperatures.

In Fig. 5 two distributions measured for copper

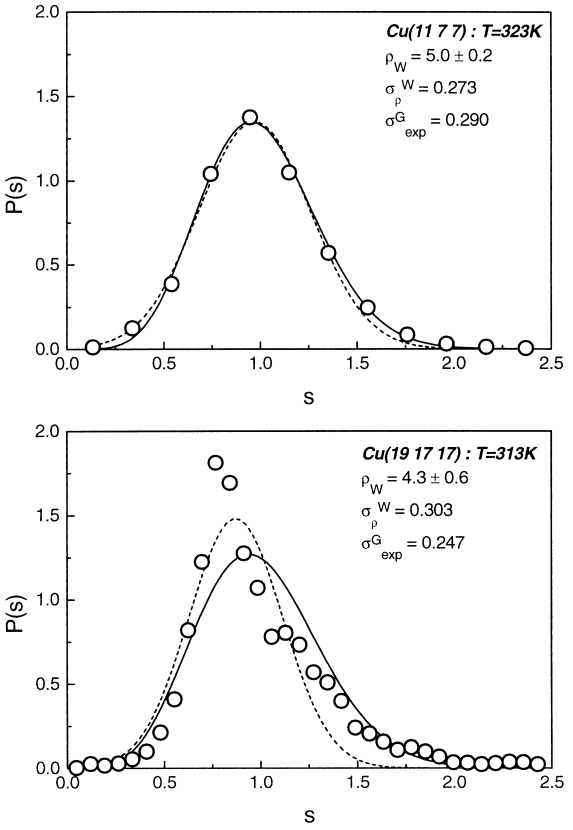


Fig. 5. TWD measured for two Cu (111) vicinal surfaces. The upper panel shows 'good' data, and the lower shows 'poor' data. The solid and dashed curves are fits to the data using the (single-parameter) Wigner and the Gaussian expressions respectively. The fitted value $\sigma^G_{exp}$ and the value $\sigma^W_\varrho$ deduced from the fitted $\varrho$ are indicated.

(111) vicinal surfaces are compared: (a) 'good' data from the (11 7 7) plane and (b) what turns out to be 'poor' data from the (19 17 17) surface. In addition we show the variance from using Eqs. (7), (11) and (12) and the variance obtained from the Gaussian fit respectively in both panels in Fig. 5. In the top panel both the GWD and the Gaussian approximation provide good agreement with the experimental data. The variances determined using the two models agree nicely: their difference is less than 4%, comparable to that due to typical experimental errors (3–6%). Such errors can be caused by slight deviations of the experimental TWD from the true equilibrium distribution due to various types of noise, sampling errors,

etc. Even when there is no obvious evidence of noise in the data, deviations of this nature must be expected. In the lower panel of Fig. 5 the TWD measured on (19 17 17) is a double-peak distribution and is obviously not well described by either of the fitting functions.

Table 2 gives an overview of our data obtained by analyzing TWDs measured on various copper vicinal surfaces as a function of the temperature. Referring to Fig. 5, the column labeled $Q$ indicates a visual assessment of the quality of each TWD. All cases with 'good' (+) data are included, along with representative cases of 'poor' (−) and of 'okay' (0) data. As shown in Fig. 4, the TWD for Cu (1 1 13) becomes broader and more asymmetric as temperature increases. In Table 2 we see for each misorientation a monotonic — to within error bars — decrease in the value of $\varrho$ with increasing temperature, as is expected from Eq. (1) and subsequent discussion. For the Cu(11 7 7) surface, no such monotonic decrease in $\varrho$ is observed. This is probably due to a systematic shift in the peak position of the normalized experimental TWDs (measured for this sample) compared with the Wigner fit, which might introduce errors into the analysis.

Considering all surfaces, we obtain values of $\varrho$ between 3.5 and 8.6. The lower end, occurring at higher temperatures, corresponds to interactions weaker than the calibration point at $\varrho=4$, near the lower limit of viable Gaussian approximations for moderate-to-strong dimensionless repulsion [3], still far from the free fermion limit and even the weak-interaction regime. Near $\varrho=4$, there is considerable numerical evidence that the GWD should describe the data well, provided the viability of fundamental assumptions such as pure inverse-square decay of energetic repulsions (even at small spacings $\ell$) and interactions only normal to the mean step direction (viz. at the same time for fermions evolving along their world lines). For lower temperatures, the dimensionless interaction on copper is more strongly repulsive, corresponding to $\varrho$ well above four.

For values of $\varrho$ below 3.5, the Gaussian approximation is expected not to provide an adequate fit to the TWD, whereas the GWD should be excellent [3]. In order to explore this limit for copper vicinals, one would have to measure step–step distance distributions at higher temperatures than shown here. This process, however, would require samples with a larger mean terrace width (i.e. smaller misorientation): with increasing temperature, the equilibrium fluctuations of steps increase. When the mean amplitude of these fluctuations is of the order of half the step separation, it becomes difficult (if not impossible) to distinguish positions of adjacent steps. This is due to the temporal information in the STM images for higher temperatures [12], which causes the steps to appear in STM images as if they crossed. Alternatively one could make use of faster STM instruments. To extend the temperature range in the case of copper to $T=500$ K, one would need a high-speed STM that is capable of recording high-resolution images at video frequency (which one can easily estimate assuming the diffusion barrier along steps to be of order 0.5 eV for Cu(001) [15]). For the present measurements on copper surfaces, 370 K is the upper limit for the determination of step positions. Even for $T=$ 320 K the data reflect a great deal of temporal rather than spatial information due to the limited speed of the STM tip [12]. Use of samples with lower step densities invites a new restriction: residual pinning sites at step edges. Residual pinning sites exert greater influence on the TWD as the mean step separation increases, making it more challenging to measure equilibrium distributions. In terms of the 'quality' of the data (col. 2), we note that for small misorientation (large Miller indices) and to some degree for higher $T$, there is a greater tendency for TWDs to be 'poor'.

In col. 5 we list the standard deviation $\sigma_\varrho^{\mathrm{W}}$ to be expected from the tabulated $\varrho$, assuming the validity of the GWD — specifically Eq. (11) [with $b_\varrho$ from Eq. (8) and the general relation Eq. (12)]. Evidently $\sigma_\varrho^{\mathrm{W}}$ (col. 5) and $\sigma_{\mathrm{exp}}^{\mathrm{G}}$ (col. 4) determined from the Gaussian fit are in reasonably good agreement for all values of $\varrho$ (see Table 2) measured in our experiments, with $\sigma_\varrho^{\mathrm{W}}$ generally larger (but rarely by over 10% and typically much less). Notably this is seen even when the peak of the Gaussian is not exactly positioned at $s=1$ due to noise in the experimental data in the peak area. In other words, the determination of the variance

Table 2
Compendium of results for various copper vicinal surfaces at different temperatures $T$ (K). The third column indicates the subjective quality of the data (see Fig. 3): 'good' (+), okay (0), or 'poor' (−). The next two columns give the results of fits to the two single-parameter expressions, the exponent $\varrho$ of the generalized Wigner surmise [Eq. (6)] and the standard deviation $\sigma$ of a Gaussian [Eq. (3)]. For comparison with the latter, we tabulate $\sigma^{W}_{\varrho}$, the value of $\sigma$ expected for a Wigner distribution [Eqs. (11) and (12) with the tabulated $\varrho$, and $\sigma(\mu_2')$, the corresponding root of the variance obtained from a direct determination of the second moment of the experimental TWDs [Eq. (11)]. Columns 8–12 give the dimensionless interaction strength [Eq. (1)] determined from the Wigner viewpoint [$\tilde{A}_W$, Eq. (7)]; from Gaussian fits interpreted based on the Gruber–Mullins approximation [$\tilde{A}_G$, Eq. (5)], continuum roughening theory [$\tilde{A}_R$, Eq. (13)], or inclusion of entropic repulsion in only an average way [$\tilde{A}_E$, Eq. (13)]; and from a measure of the TWD skewness [$\tilde{A}_{hw}$, Eq. (15)] to extract an estimate of $\varrho$, then Eq. (12)]. The temperature dependence of $T^2A_W$ and of $T^2A_G$ is primarily that of the step-edge stiffness [Eq. (1)] and is given in $10^6K^2$. The interaction constants $A_W$ and $A_G$ are given in units of meV Å, where (see Footnote 1) $\epsilon=110$ meV, $a_\perp=2.21$ Å and $a_\parallel=2.55$ Å for the Cu(111) vicinal surfaces and $\epsilon=128$ meV, $a_\perp=a_\parallel=2.55$ Å for the Cu(100) vicinals

| Column | 1 | 2 | 3 | 4 | 5 | 6 | 7 | 8 | 9 | 10 | 11 | 12 | 13 | 14 | 15 | 16 | 17 |
|---|---|---|---|---|---|---|---|---|---|---|---|---|---|---|---|---|---|
| Surface | $T$ (K) | $Q$ | $\varrho$ | $\sigma^{G}_{exp}$ | $\sigma^{W}{}_{\varrho}$ | $\sigma(\mu_2')$ | $\tilde{A}_W$ | $\tilde{A}_G$ | $\tilde{A}_R$ | $\tilde{A}_E$ | $\tilde{A}_{hw}$ | $T^2\tilde{A}_W$ | $T^2\tilde{A}_G$ | $A_W$ | $A_G$ | $A_R$ | $A_E$ |
| Cu (1 1 7) | 298 | + | 8.6±0.5 | 0.208±0.007 | 0.196 | 0.203 | 14.2±1.9 | 10.3 | 17.2 | 24.6 | 26.9 | 1.26 | 0.91 | 12.9±1.7 | 9.3±1.3 | 15.6 | 22.3 |
| Cu (1 1 13) | 285 | + | 8.4±0.7 | 0.193±0.011 | 0.198 | 0.246 | 13.4±2.6 | 13.9 | 24.1 | 34.3 | 31.0 | 1.09 | 1.09 | 9.3±1.8 | 9.6±2.2 | 16.6 | 23.6 |
| | 295 | + | 7.5±0.2 | 0.245±0.007 | 0.212 | 0.231 | 10.3±0.7 | 5.3 | 8.0 | 11.7 | 10.7 | 0.90 | 0.46 | 8.8±0.6 | 4.6±0.5 | 6.8 | 10.0 |
| | 300 | + | 6.4±0.5 | 0.249±0.011 | 0.233 | 0.277 | 7.0±1.4 | 5.0 | 7.4 | 10.8 | 2.3 | 0.63 | 0.45 | 6.6±1.3 | 4.7±0.8 | 7.0 | 10.2 |
| | 320 | + | 5.2±0.5 | 0.264±0.012 | 0.266 | 0.326 | 4.2±1.1 | 4.0 | 5.5 | 8.2 | 6.2 | 0.43 | 0.41 | 5.7±1.4 | 5.4±1.0 | 7.6 | 11.3 |
| | 338 | + | 5.3±0.6 | 0.253±0.010 | 0.263 | 0.336 | 4.4±1.3 | 4.7 | 6.8 | 10.1 | 7.3 | 0.50 | 0.54 | 8.2±2.4 | 8.8±1.4 | 12.8 | 18.9 |
| | 348 | + | 4.4±0.6 | 0.265±0.014 | 0.298 | 0.340 | 2.6±1.0 | 3.9 | 5.4 | 8.1 | 5.6 | 0.31 | 0.47 | 5.8±2.2 | 8.6±1.8 | 11.9 | 17.8 |
| Cu (1 1 19) | 320 | + | 6.6±0.3 | 0.254±0.008 | 0.229 | 0.257 | 7.6±0.8 | 4.6 | 6.7 | 9.9 | 7.7 | 0.78 | 0.47 | 10.5±1.2 | 6.4±0.8 | 9.2 | 13.7 |
| | 360 | + | 5.7±0.4 | 0.266±0.013 | 0.251 | 0.284 | 5.3±0.9 | 3.8 | 5.3 | 7.9 | 6.6 | 0.68 | 0.50 | 13.9±2.5 | 10.1±2.0 | 14.0 | 20.8 |
| | 370 | – | 4.1±0.7 | 0.254±0.033 | 0.314 | 0.304 | 2.2±1.1 | 4.6 | 6.7 | 9.9 | 3.2 | 0.29 | 0.63 | 6.5±3.3 | 14.1±9.7 | 20.4 | 30.1 |
| Cu (11 7 7) | 296 | + | 9.9±0.5 | 0.162±0.003 | 0.181 | 0.190 | 19.6±2.2 | 27.9 | 51.8 | 72.8 | – | 1.71 | 2.45 | 26.3±4.0 | 37.7±7.5 | 69.8 | 98.1 |
| | 301 | + | 6.0±0.4 | 0.265±0.004 | 0.243 | 0.281 | 6.0±1.0 | 3.9 | 5.4 | 8.1 | 7.9 | 0.54 | 0.35 | 8.8±2.0 | 5.8±1.3 | 8.0 | 11.9 |
| | 306 | + | 4.8±0.4 | 0.276±0.001 | 0.304 | 0.364 | 3.4±0.8 | 3.3 | 4.4 | 6.6 | 5.4 | 0.31 | 0.31 | 5.4±1.6 | 5.3±0.9 | 7.1 | 10.6 |
| | 323 | + | 5.0±0.2 | 0.290±0.008 | 0.273 | 0.316 | 3.8±0.4 | 2.7 | 3.4 | 5.2 | 4.4 | 0.39 | 0.28 | 8.0±1.1 | 5.8±0.7 | 7.3 | 11.1 |
| Cu (19 17 17) | 313 | – | 4.3±0.6 | 0.247±0.014 | 0.303 | 0.381 | 2.5±1.0 | 5.2 | 7.7 | 11.3 | 5.3 | 0.24 | 0.51 | 4.5±2.3 | 9.4±2.3 | 14.0 | 20.5 |
| | 333 | −/0 | 3.7±0.4 | 0.324±0.015 | 0.339 | 0.361 | 1.6±0.5 | 1.7 | 1.8 | 2.9 | 0.6 | 0.17 | 0.19 | 3.9±1.8 | 4.3±1.0 | 4.5 | 7.2 |
| | 353 | −/0 | 4.0±0.3 | 0.314±0.013 | 0.319 | 0.333 | 2.0±0.5 | 2.0 | 2.2 | 3.4 | 1.2 | 0.25 | 0.25 | 6.6±2.0 | 6.6±1.1 | 7.3 | 11.3 |
| Cu (23 21 21) | 328 | 0 | 5.3±0.3 | 0.288±0.009 | 0.263 | 0.310 | 4.4±0.6 | 2.8 | 3.5 | 5.3 | 5.2 | 0.47 | 0.30 | 10.1±2.0 | 6.5±0.8 | 8.1 | 12.2 |

using a three-parameter Gaussian fit remains reliable for shifted and slightly asymmetric distributions. Hence, the Gaussian analysis also provides excellent results for the variances and the interaction constants when an experimental distribution is not normalized with respect to the mean terrace width and unit mean, and so is more forgiving than the one-parameter Wigner approach.

Following suggestions in EP [3] we have also determined directly and explicitly the second and the third moments of the experimental distributions [Eq. (10)]. We discuss $\mu_3'$ below in the context of skewness. From the second moment about the origin, we tabulate the corresponding standard deviation $\sigma(\mu_2')$ via Eq. (12). In many cases $\sigma(\mu_2')$ (col. 6) agrees well with $\sigma_{\varrho}^{\mathrm{W}}$ and $\sigma_{\mathrm{exp}}^{\mathrm{G}}$, but in a few cases it is considerably larger or smaller. The scattering in the results for the second moment is due to noise in the experimental data. Even with the relatively large database of our experiments, the evaluation of $\mu_2'$(exp) depends sensitively on the noise of the data. Hence, simple direct determination of the second moment from an experimental distribution is not a reliable method to obtain information about $\varrho$ and the step–step interaction.

Having found decent agreement of the variances deduced from the Wigner and the Gaussian analyses, we next tabulate the associated dimensionless interaction strengths based on competing approximation schemes. In the Wigner framework, $\tilde{A}_{\mathrm{W}}$ comes immediately from the fitted $\varrho$ via Eq. (7) (col. 7). Columns 7–11 give the value of $\tilde{A}$ deduced pursuant to several perspectives from the (same) standard deviation $\sigma_{\mathrm{exp}}^{\mathrm{G}}$ of a Gaussian fit. The standard Gruber–Mullins single-active-step result is given by $\tilde{A}_{\mathrm{G}}$; here we use the expression derived for interactions between all steps [Eq. (5)] rather than the conventionally invoked expression for just nearest-neighbor-step repulsions [Eq. (4)]. For smaller values of the dimensionless interaction strength ($\tilde{A}<5$) the agreement between $\tilde{A}_{\mathrm{G}}$ and $\tilde{A}_{\mathrm{W}}$ is generally good, whereas for large values ($\tilde{A}>7$) $\tilde{A}_{\mathrm{G}}$ is generally smaller than $\tilde{A}_{\mathrm{W}}$. In the discussions by the Grenoble [4,5] and Saclay [6–8] groups of the shortcomings of the Gruber–Mullins perspective, it was not evident how large the dimensionless interaction strength must be for the underestimation of it by Eqs. (4) or (5) to become apparent. From the tabulation we see that, over our experimental range of dimensionless interaction strengths, the results stemming from the vantage of roughening theory $\tilde{A}_{\mathrm{R}}$ are mostly much closer to $\tilde{A}_{\mathrm{W}}$ than those approximating the entropic repulsion $\tilde{A}_{\mathrm{E}}$ (which presumably are the most accurate for asymptotically large interactions). Even though $\varrho_{\mathrm{E}}/\varrho_{\mathrm{R}}$ is just $\kappa_{\mathrm{E}}/\kappa_{\mathrm{R}}=1.17$, we find [with Eq. (13)] that $\tilde{A}_{\mathrm{E}}/\tilde{A}_{\mathrm{R}}\approx 1.5\pm 0.1$. If the entropic repulsion is neglected completely [4,5], then the analogous ratio $\tilde{A}_{\mathrm{E0}}/\tilde{A}_{\mathrm{R}}$ is even larger, around two.

Column 11 in Table 2 concerns fitting the asymmetry of the half widths at half maximum. Our approach, as noted in Section 3.4, was first to smooth the data by fitting to the generalized Wigner expression taken as a three-parameter function, with $a$ and $b$ not fixed by normalization and unit-mean conditions. From the fitted form we obtained the half widths $w_+$ and $w_-$, then used Eq. (15) to determine the skewness $\alpha_3^{\mathrm{hw}}$ and thence the value of $\tilde{A}_{\mathrm{hw}}$.[10]

Finally, we explore some consistency checks of the dimensionless interaction strength: we have tabulated the values for $T^2\tilde{A}_{\mathrm{W}}$ and $T^2\tilde{A}_{\mathrm{G}}$ in units of $10^6\mathrm{K}^2$ (cols 12, 13). From Eq. (1) and assuming that the elastic repulsion between steps to be relatively insensitive to temperature, we expect this quantity to have the same $T$ dependence as the step stiffness $\tilde{\beta}$. Fig. 6 shows $T^2\tilde{A}_{\mathrm{W}}$ and $T^2\tilde{A}_{\mathrm{G}}$ for the complete data set obtained for Cu (1 1 13). The solid circles and open squares are the experimental data obtained from $\tilde{A}_{\mathrm{W}}$ and $\tilde{A}_{\mathrm{G}}$ respectively, and the solid curve is the scaling prediction embodied in Eq. (1), with $\tilde{\beta}$ computed as specified in Footnote 4 and $A_{\mathrm{G}}=7.1$ meV Å as found in Ref. [9]. Considering the error bars introduced by

[10] The drawback of this method, at least as presently implemented and for the range of the dimensionless interaction considered, comes from sensitivity in fitting the TWD to get half widths, not in then using Eq. (15). Although our extracted $\tilde{A}_{\mathrm{hw}}$ is consistently too large, it does display the correct trend, and so might serve as a general check. The unmet challenge is to assess the skewness without in essence fitting the whole TWD. Attempts to determine the skewness by computing $\mu_3'$ directly from the data [following Eq. (10)] were futile. Noise had a more dramatic effect than for $\mu_2'$, sometimes producing a negative value for $\mu_3$ and so the skewness. Therefore, we have not listed the third moments or their equivalents in Table 2.

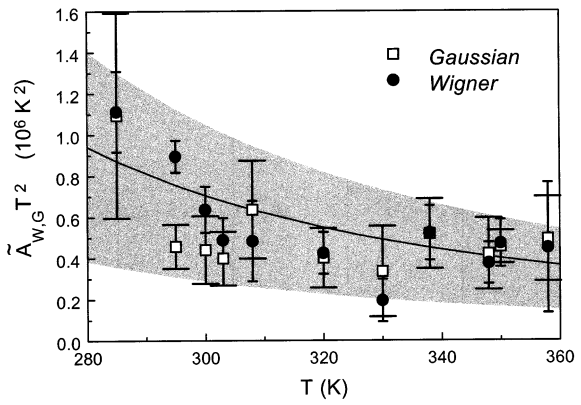


Fig. 6. Temperature dependence of $T^2\tilde{A}_W$ (solid circles) and $T^2\tilde{A}_G$ (open squares) for Cu (1 1 13), with error bars distinguished by narrow and wide feet respectively. The solid curve is calculated from Eq. (1), with $\tilde{\beta}$ obtained from Footnote 4 and $A$ set to 7.1 meV Å, the value determined in Ref. [9]. The gray band blanketing the data corresponds to a range of about $\pm 50\%$ of $A$.

the error of $\tilde{A}_W$ and of $\tilde{A}_G$ (as given in Table 2), the experimental data satisfy the predicted thermal scaling behavior. The error bars of $\pm 3.8$ meV Å quoted in Ref. [9] are fortuitously similar to the bounds of the gray region in Fig. 6, $7.1^{+3.5}_{-4.2}$ meV Å, that blanket the data.

We now invert this approach, assuming the validity of Eq. (1) and use it as a test. Even though the quality of the Gaussian fit to TWDs may be comparable or somewhat better than the Wigner fit, extraction of $\tilde{A}$ from $\sigma^G_{exp}$ can be problematic since the optimal prefactor of the Gaussian depends on $\tilde{A}$. (E.g. the $\tilde{A}_E$ estimate should be more accurate than the $\tilde{A}_R$ estimate at high $\tilde{A}$, or low temperature.) In the case of Cu (1 1 13), for which we made measurements at most temperatures, Fig. 6 shows that the Gaussian data are not particularly worse than the Wigner data. By removing the stiffness as well as the thermal energy from $\tilde{A}_W$ and $\tilde{A}_G$, we extract the physical amplitudes $A_W$ and $A_G$ of the elastic repulsion, which have dimensions [energy]×[length]. Separate fits to the Gaussian (from Gruber–Mullins perspective) and to the Wigner data give estimates $\langle A_G\rangle = 6.9$ meV Å and $\langle A_W\rangle = 7.2$ meV Å, the angular brackets indicating that these estimates are based on several different temperatures, unlike earlier estimates. Combining both sets, we determine $A = 7.1 \pm 0.5$ meV Å. Recall that the close agreement here between these two estimates is exceptional; more generally for this system, Table 2 indicates that the Wigner estimate of the interaction strength ($A_W$; col. 14) is closer to the value of the interaction strength extracted from the experimental Gaussian width assuming the roughening picture advanced by the Saclay group ($A_R$; col. 16). The expectation of thermal insensitivity is somewhat better realized by $A_G$ extracted from $T^2\tilde{A}_G$ than by the corresponding $A_W$ (Table 2), as measured by a somewhat smaller standard deviation of their average. Moreover, one expects $A$ not to depend on the misorientation angle for a given terrace plane, at least for small angles. The sizeable variability gives a powerful indication of the difficulty in extracting quantitative estimates of the elastic repulsion.

## 5. Conclusions and summary

We have seen that for vicinal copper surfaces at temperatures near and within $\sim 50$ K above room temperature, the dimensionless interaction can be characterized as moderately strong. In the weak regime, the Gaussian approximation would provide a poor fit to highly skewed TWDs.[11] In the very strong regime, the interaction strength would likely be extractable using the asymptotic expression for $\tilde{A}_E$ in Eq. (13). For the present experiments, we find that both the Wigner and the Gaussian fits provide adequate accounts of the data. The Wigner form captures the notable skewness at smaller $\tilde{A}$ values and by virtue of the excellent agreement with the exact results at $\varrho = 4$, should be particularly accurate for the cases of weaker $\tilde{A}$ values we studied. Even if it were easier to extract Gaussian widths than to fit to the generalized Wigner form, the interpretation of these widths has become problematical. Since $\tilde{A}$

[11] Experiments in such a regime were recently reported for vicinal Pt(110) [28]; the data beg analysis with the generalized Wigner surmise, from which we [25] obtain a quantitative rather than a qualitative estimate of the interaction of the apparent weak step–step repulsion.

depends on the fourth power of this width, while only quadratically on $\varrho$, the error seems to be somewhat amplified in the Gaussian fit. More seriously, there is controversy over the optimal choice of prefactor when analyzing the Gaussian width, as discussed in Section 3.3 (cf. Table 1). For the present range of dimensionless interactions, the value derived by the Saclay group based on roughening theory arguably gives the best overall estimate of $\tilde{A}$ from the Gaussian width. However, Monte Carlo tests [29] provide evidence that the GWD offers a superior estimate, not just between the values of $\tilde{A}$ for which exact solutions exist, but throughout the physical range of $\tilde{A}$ and beyond. Moreover, for large $\varrho$ the GWD tends toward a Gaussian; Ref. [25] provides a quantitative analysis of this approach. Furthermore, a straightforward expression has been developed [25] to go from the variance of the GWD as given in Eq. (11) to $\tilde{A}$ without an implicit inversion $b_\varrho$ as given in Eq. (8).

We have learned many practical lessons regarding analysis of data in light of the EP [3] results. The direct determination of the moments of TWDs generally offers little reliable information on actual TWDs due to large errors caused by noise in the experimental data. Although the skewness of the TWD should provide a useful measure for weak interactions, it is not clear how to fit conveniently to get quantitative information without going to the full Wigner expression, thereby obviating the need to monitor the skewness separately. In fitting to the Wigner expression, the most pressing concern is to devise ways to minimize the sensitivity to uncertainty in the local average step separation. When this fitting is performed in the two parameters $\varrho$ and (an adjustment factor to) $\langle\ell\rangle$, the value of $\varrho$ typically changes insignificantly for 'good' data but can increase substantially (of order 5–20%) for bad data [25]. Invariably, in the latter case the fitted $\langle\ell\rangle$ is less than one expects from the raw data (e.g. the first moment), by of order 8%. In other words, when $\ell$ is converted to $s$ using the measured average step–step-separation $\langle\ell\rangle$, the mean of $P_\varrho(s)$ determined from the two-parameter fit is larger than one [25].

In a more general point of view, our results, particularly as presented in Table 2, serve as a sobering warning about the level of accuracy one can presently hope to achieve in gauging the strength of the elastic repulsion, especially for a limited set of measurements. While evidently this strength deduced from the traditional Gruber–Mullins approach ($A_G$) is systematically much lower than that deduced from the Wigner formalism for lower temperatures (larger $\tilde{A}$), another pervasive problem is the unexpected variability of $A$ under changes of temperature or misorientation. Presumably this is a measure of the noise in the measurement process. It appears to be optimistic to believe that one can measure $A$ for this sort of system to within better than 5–10% accuracy; error bars several times larger may often be more realistic. When accurate probing of $A$ is needed, one should measure several temperatures and misorientations to check stability and reliability.

Furthermore, all analyses rely on the approximation that the repulsion between steps occurs only perpendicular to their mean direction (which corresponds to instantaneous interactions between pairs of fermions) and take as given the $A/\ell^2$ repulsion. Both may well break down at small $\ell$ or large fluctuations. However, it has been noted already that measurements in this regime are problematical, so that issue may not pose a significant obstacle in approaching good data. As discussed in Ref. [3], there are further assumptions, often unrealistic, needed to deduce a surface stress responsible for the value of $A$.

## Acknowledgements

We gratefully acknowledge H. Ibach for helpful discussions and detailed comments on the manuscript. MG thanks U. Linke for skillful sample preparation. TLE also benefited greatly from collaboration with O. Pierre-Louis on this subject. He thanks N.C. Bartelt for the program used to compute the exact form in Fig. 2 and for helpful remarks and S.D. Cohen, H.L. Richards, and E.D. Williams for useful comments. TLE gratefully acknowledges support for his research from NSF MRSEC grant DMR 96-32521; furthermore, he recognizes with gratitude the support of a

Humboldt U.S. Senior Scientist Award and the hospitality of the IGV at FZ-Jülich.

## References

[1] E.E. Gruber, W.W. Mullins, J. Phys. Chem. Solids 28 (1967) 875.
[2] N.C. Bartelt, T.L. Einstein, E.D. Williams, Surf. Sci. 240 (1990) L591.
[3] T.L. Einstein, O. Pierre-Louis, Surf. Sci. 424 (1999) L299.
[4] O. Pierre-Louis, C. Misbah, Phys. Rev. B 58 (1998) 2265.
[5] T. Ihle, C. Misbah, O. Pierre-Louis, Phys. Rev. B 58 (1998) 2289.
[6] L. Masson, L. Barbier, J. Cousty, B. Salanon, Surf. Sci. 317 (1994) L1115.
[7] L. Barbier, L. Masson, J. Cousty, B. Salanon, Surf. Sci. 345 (1996) 197.
[8] E. LeGoff, L. Barbier, L. Masson, B. Salanon, Surf. Sci. 432 (1999) 139.
[9] M. Giesen, Surf. Sci. 370 (1997) 55.
[10] M. Giesen, G.S. Icking-Konert, Surf. Rev. Lett. 6 (1999) 27.
[11] M. Giesen, U. Linke, H. Ibach, Surf. Sci. 389 (1997) 264.
[12] M. Giesen-Seibert, F. Schmitz, R. Jentjens, H. Ibach, Surf. Sci. 329 (1995) 47.
[13] M. Poensgen, J.F. Wolf, J. Frohn, M. Giesen, H. Ibach, Surf. Sci. 274 (1992) 430.
[14] N.C. Bartelt, T.L. Einstein, E.D. Williams, Surf. Sci. 276 (1992) 308.
[15] M. Giesen-Seibert, H. Ibach, Surf. Sci. 316 (1994) 205.
[16] G. Schulze Icking Konert, M. Giesen, H. Ibach, Phys. Rev. Lett. 83 (1999) 3880.
[17] B. Joós, T.L. Einstein, N.C. Bartelt, Phys. Rev. B 43 (1991) 8153.
[18] B. Sutherland, J. Math. Phys. 12 (1971) 246.
[19] M.L. Mehta, Random Matrices, second ed., Academic, New York, 1991.
[20] T. Guhr, A. Müller-Groeling, H.A. Weidenmüller, Phys. Rep. 299 (1998) 189.
[21] P.J. Forrester, Nucl. Phys. B 388 (1992) 671.
[22] F.D.M. Haldane, in: A. Okiji, N. Kawakami (Eds.), Correlation Effects in Low-Dimensional Electronic Systems, Springer, Berlin, 1994, p. 3.
[23] Z.N.C. Ha, Nucl. Phys. B 435 (1995) 604.
[24] E.W. Plummer, personal communication.
[25] H.L. Richards, S.D. Cohen, T.L. Einstein, M. Giesen, Surf. Sci. (2000) in press.
[26] J. Frohn, M. Giesen, M. Poensgen, H. Ibach, Phys. Rev. Lett. 67 (1991) 3543.
[27] J.W.M. Frenken, P. Stoltze, Phys. Rev. Lett. 82 (1999) 3500.
[28] K. Swamy, E. Bertel, I. Vilfan, Surf. Sci. 425 (1999) L369.
[29] S.D. Cohen, H.L. Richards, T.L. Einstein, Bull. Am. Phys. Soc. 45 (2000) talk M31.05, unpublished.